6th European Conference on Computational Mechanics (ECCM 6)
7th European Conference on Computational Fluid Dynamics (ECFD 7)
11-15 June 2018, Glasgow, UK

CONCRETE FATIGUE MODEL BASED ON CUMULATIVE INELASTIC SHEAR STRAINS

Abedulgader Baktheer[1], Josef Hegger[1] and Rostislav Chudoba[1]

[1] Institute of Structural Concrete, RWTH Aachen University
Mies-van-der-Rohe-Straße 1 , 52074 Aachen , Germany
Abaktheer@imb.rwth-aachen.de
www.imb.rwth-aachen.de

Key words: Concrete fatigue, Constitutive modeling, Microplane theory, Thermodynamics

Abstract. In this paper, we introduce a thermodynamic based microplane fatigue damage model for plain concrete. The key idea of this approach is to relate the fatigue damage to a cumulative measure of inelastic sliding/shear strains. Which reflects the fatigue damage accumulation owing to internal friction under subcritical fatigue loading. The model is formulated within the microplane framework using a homogenization approach based on the energy equivalence principal with explicit representation of the elastic stiffness. The model can reflect the triaxial behavior of concrete and model the hysteric loops with the relation to the fatigue damage propagation of concrete at the macroscopic material representation. Elementary studies of the model response and its applicability to modeling the fatigue behavior of concrete under compression are presented.

1 INTRODUCTION

The concern about the effect of fatigue on concrete structures has increased in the last decades due to the design of more slender concrete elements. The limited warning alert of the brittle fatigue failure increasing the importance of studying the behavior of concrete under fatigue loading. Characterization of concrete fatigue behavior is a challenging task that has increasingly attracted the attention of researchers during the past decades. Besides extensive experimental investigations, several attempts have been made to develop reliable numerical models. However, for concrete, the underlying microstructural mechanisms governing concrete fatigue damage propagation are still not sufficiently understood.

Several models addressing the concrete fatigue damage propagation have been proposed in the literature. Pragmatic approaches to modeling use the number of performed loading cycles directly as a damage driving variable [1]. More advanced approaches to simulation of fatigue damage process cycle by cycle at subcritical load levels with damage related either to total strain [2, 3], or to the inelastic strain [4]. In order to reflect the opening/closure and growth of microcracks and/or the frictional sliding along their

lips, the formulation of the dissipative mechanisms has been refined by introducing the internal sliding strain as a fatigue damage driving variable [5]. An approach relating the dissipative terms owing to fatigue damage even closer to the observable disintegration mechanisms within the material structure appeared recently in [6]. The key idea of this model is to relate the damage evolution to the cumulative measure of volumetric strain.

Microplane model formulation can be regarded as a coupled multiscale model. Indeed, it introduces an additional level of state representation below the level of material point. Even though this level does not have the ambition to reflect the spatial layout of the material microstructure, it can reflect a damage pattern and its anisotropic evolution during the loading in a smeared way. It applies the concept of kinematic constraint and stress homogenization in order to establish a link between the macroscopic and microplane level of discretization [7, 8].

Fatigue damage developing at subcritical load levels includes several interacting mechanisms: development of coalescence of microcracks, repeated crack opening and closure, internal sliding and friction. The roughness of cracked surfaces and the interlocking of aggregates generates inelastic strain and impose friction sliding of the microcracks lips and aggregates. It is important for fatigue modeling to consider the inelastic dissipation owing to damage (development of microcracks) and internal frictional sliding (within the deteriorating structure). In spite of the progress in the development of numerical phenomenological material models of fatigue, there is a need to formulate an appropriate damage hypotheses taking into account the aforementioned mechanisms governed the ac-

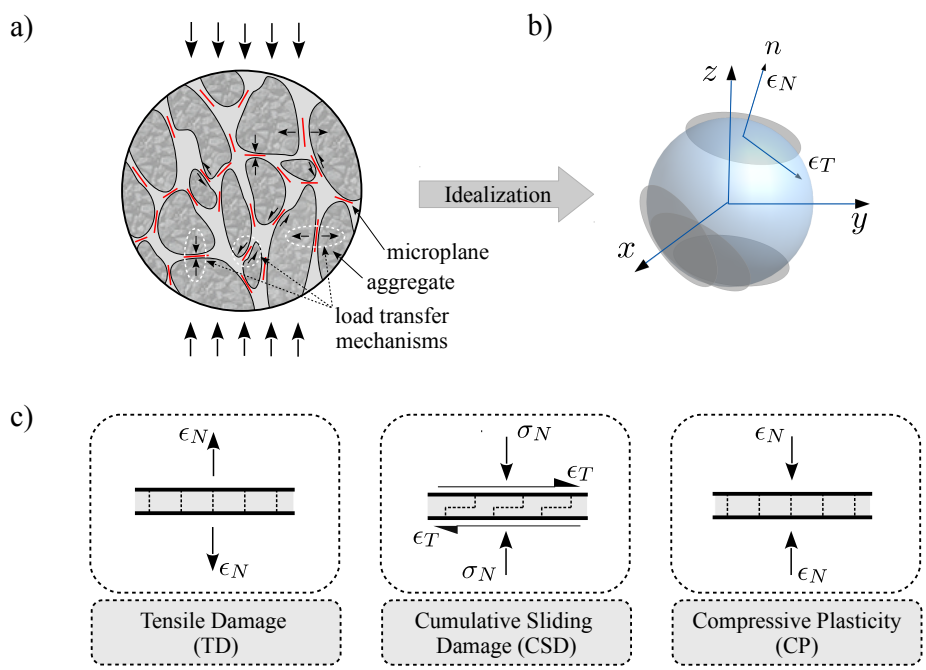

Figure 1: Dissipative mechanisms of the proposed microplane model: a) example of idealized microstructure with system of assumed microplanes and the load transfer mechanisms under compression loading; a) microplane directions; c) dissipative mechanisms

cumulation of damage due to fatigue loading. The framework provided by the microplane model is ideally suited for reflecting the microscopic interaction of normal and pressure sensitive friction dissipative mechanisms see Fig 1.

In this paper we introduce a thermodynamically based microplane fatigue damage model for plain concrete. The key idea of this model is to relate the fatigue damage to a cumulative measure of inelastic sliding/shear strains. Which reflects the fatigue damage accumulation owing to internal friction under subcritical fatigue loading.

2 MODEL FORMULATION

Unlike the classical constitutive models where the stress and strain tensors are related directly, the microplane models work with stress and strain vectors at the planes with various directions (microplanes). The strain tensor is projected into the oriented microplanes, then the constitutive laws are evaluated at each microplane, finally the stress tensor is obtained by the integration over all microplanes. The skeleton of the model formulation is presented in Fig 2.

2.1 Kinematic constraint

The strain tensor is projected onto the microplane to obtain strain vectors i.e. normal and tangential direction with the so called kinematic constraint as follows

$$\varepsilon_{\mathrm{N}} = \boldsymbol{N} : \boldsymbol{\varepsilon}, \qquad \boldsymbol{\varepsilon}_{\mathbf{T}} = \mathbf{T} : \boldsymbol{\varepsilon}, \tag{1}$$

where the scalar ε_{N} is the normal microplane strain, and $\boldsymbol{\varepsilon}_{\mathbf{T}}$ is the tangential microplane vector. The second order normal tensor $\boldsymbol{N}$ and the third order tangential tensor $\boldsymbol{T}$ are given as

$$\boldsymbol{N} = \boldsymbol{n} \otimes \boldsymbol{n}, \qquad \mathbf{T} = \boldsymbol{n} \cdot \mathbb{I}_{sym} - \boldsymbol{n} \otimes \boldsymbol{n} \otimes \boldsymbol{n}, \tag{2}$$

where $\boldsymbol{n}$ is the microplane normal vector and $\mathbb{I}$ is the fourth-order identity tensor.

2.2 Thermodynamic based microplane constitutive laws

The constitutive laws governing the macroscopic behavior are defined on the generic microplanes. Several dissipative mechanisms are introduced in this model and illustrated in Fig 1. The corresponding macroscopic thermodynamic potential can be expressed as

$$\psi^{\mathrm{mac}} = \frac{3}{2\pi} \int_{\Omega} \psi^{\mathrm{mic}} d\Omega = \frac{3}{2\pi} \int_{\Omega} \psi^{\mathrm{mic}}_{\mathrm{N}} d\Omega + \frac{3}{2\pi} \int_{\Omega} \psi^{\mathrm{mic}}_{\mathrm{T}} d\Omega \tag{3}$$

Normal microplane constitutive law: The microplane thermodynamic potential of the normal direction is expressed as

$$\rho\psi^{\mathrm{mic}}_{\mathrm{N}} = \frac{1}{2}\left[1 - H(\sigma_{\mathrm{N}})\,\omega_{\mathrm{N}}\right] E_{\mathrm{N}}(\varepsilon_{\mathrm{N}} - \varepsilon^{P}_{\mathrm{N}})^2 + \frac{1}{2} K_{\mathrm{N}} z^2_{\mathrm{N}} + \frac{1}{2}\gamma_{\mathrm{N}} \alpha^2_{\mathrm{N}} + f(r_{\mathrm{N}}), \tag{4}$$

where $\psi^{\mathrm{mic}}_{\mathrm{N}}$ is the Helmholtz free energy of the normal direction, ρ is the density, the normal elastic stiffness is $E_{\mathrm{N}} = E/(1-2\nu)$, where E is the Young modulus and ν is

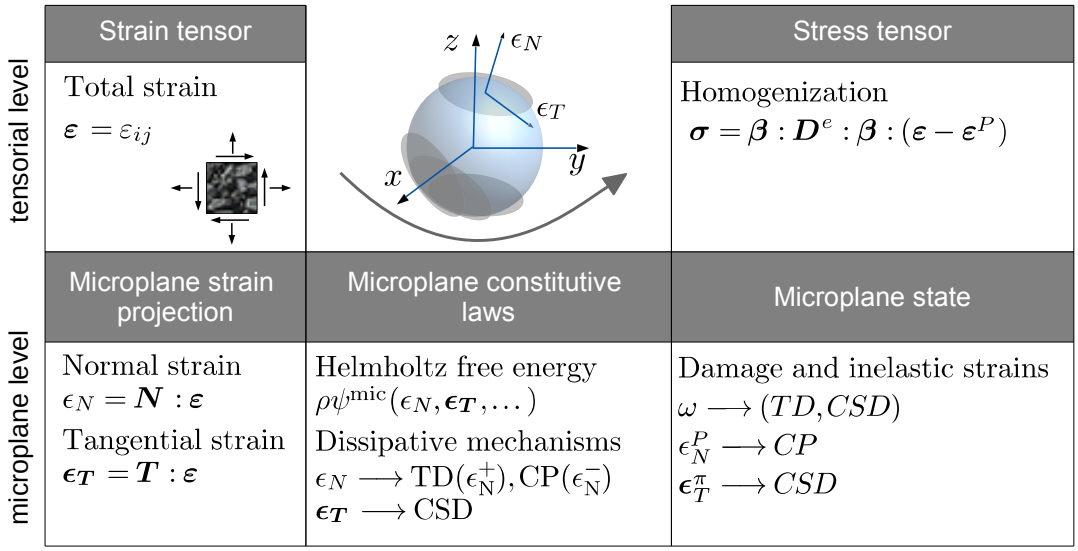

Figure 2: Approach to the formulation of the microplane model accounting for fatigue damage driven by cumulative sliding microplane strain

the Poisson's ratio. $H(\sigma_\mathrm{N})$ is a Heaviside function for switching the normal behavior i.e. damage under tension $H(\sigma_\mathrm{N}^+) = 1$, and plasticity under compression $H(\sigma_\mathrm{N}^-) = 0$, K_N and γ_N are the isotropic and kinematic hardening moduli, respectively. The thermodynamic internal variables are plastic normal strain ε_N^P defining the irreversible strain, damage variable ω_N ranging from 0 to 1, the internal variables of isotropic hardening z_N and kinematic hardening α_N. The function $f(r_\mathrm{N})$ defined a consolidation function associated with damage. The thermodynamic forces are obtained by differentiating the thermodynamic potential (4) with respect to each internal variable. Therefore, the normal stress is obtained as

$$\sigma_\mathrm{N} = \frac{\partial \rho\psi_\mathrm{N}}{\partial \varepsilon_\mathrm{N}} = \left[1 - H(\sigma_\mathrm{N})\,\omega_\mathrm{N}\right] E_\mathrm{N}(\varepsilon_\mathrm{N} - \varepsilon_\mathrm{N}^p). \tag{5}$$

The thermodynamic hardening forces can be obtained as

$$Z_\mathrm{N} = \frac{\partial \rho\psi_\mathrm{N}}{\partial z_\mathrm{N}} = K_\mathrm{N} z_\mathrm{N}, \qquad X_\mathrm{N} = \frac{\partial \rho\psi_\mathrm{N}}{\partial \alpha_\mathrm{N}} = \gamma_\mathrm{N}\alpha_\mathrm{N}, \tag{6}$$

the energy release rate owing to the damage mechanism can be defined as

$$Y_\mathrm{N} = \frac{\partial \rho\psi_\mathrm{N}}{\partial \omega_\mathrm{N}} = \frac{1}{2} H(\sigma_\mathrm{N}) E_\mathrm{N}(\varepsilon_\mathrm{N} - \varepsilon_\mathrm{N}^p)^2. \tag{7}$$

Similar to [10], the thermodynamic force associated with the damage consolidation is defined as

$$R_\mathrm{N} = \frac{\partial \rho\psi_\mathrm{N}}{\partial r_\mathrm{N}} = \frac{1}{A_\mathrm{d}} \left[\frac{-r_\mathrm{N}}{1 + r_\mathrm{N}}\right]. \tag{8}$$

where A_d is a material parameter defining the brittleness of the damage evolution. The yield function of the plasticity governed compressive behavior is given as

$$f_\mathrm{N}^p = |\tilde{\sigma}_\mathrm{N} - X_\mathrm{N}| - Z_\mathrm{N} - \sigma_\mathrm{N}^0 \leq 0, \tag{9}$$

where σ_{N}^{0} is the plastic yielding stress. The flow potential is extended by a non-associative term introducing a nonlinear hardening is given as follows

$$\phi_{\mathrm{N}}^{p} = |\tilde{\sigma}_{\mathrm{N}} - X_{\mathrm{N}}| - Z_{\mathrm{N}} - \sigma_{\mathrm{N}}^{0} + \frac{1}{2} m X_{\mathrm{N}}^{2}, \tag{10}$$

where m is the nonlinear hardening parameter. The threshold function governed the damage evolution is defined as

$$f_{\mathrm{N}}^{\omega} = Y_{\mathrm{N}} - (Y_{\mathrm{N}}^{0} + R_{\mathrm{N}}) \leq 0, \tag{11}$$

where the energy release rate threshold is $Y_{\mathrm{N}}^{0} = \frac{1}{2} E_{\mathrm{N}} (\varepsilon_{\mathrm{N}}^{0})^{2}$, $\varepsilon_{\mathrm{N}}^{0}$ is the elastic threshold normal strain. The evolution laws are obtained by differentiating the flow potential for plasticity (10) and the damage threshold function (11) with respect to the thermodynamic forces

$$\dot{\varepsilon}_{\mathrm{N}}^{p} = \dot{\lambda}_{\mathrm{N}}^{p} \frac{\partial f_{\mathrm{N}}^{p}}{\partial \sigma_{\mathrm{N}}} = \dot{\lambda}_{\mathrm{N}}^{p} \operatorname{sign}(\sigma_{\mathrm{N}} - X_{\mathrm{N}}) \tag{12}$$

$$\dot{z}_{\mathrm{N}} = -\dot{\lambda}_{\mathrm{N}}^{p} \frac{\partial f_{\mathrm{N}}^{p}}{\partial Z_{\mathrm{N}}} = \dot{\lambda}_{\mathrm{N}}^{p} \tag{13}$$

$$\dot{\alpha}_{\mathrm{N}} = -\dot{\lambda}_{\mathrm{N}}^{p} \frac{\partial f_{\mathrm{N}}^{p}}{\partial X_{\mathrm{N}}} = \dot{\lambda}_{\mathrm{N}}^{p} \left[\operatorname{sign}(\sigma_{\mathrm{N}} - X_{\mathrm{N}}) + m\, X_{\mathrm{N}}\right] \tag{14}$$

$$\dot{\omega}_{\mathrm{N}} = \dot{\lambda}_{\mathrm{N}}^{\omega} \frac{\partial f_{\mathrm{N}}^{\omega}}{\partial Y_{\mathrm{N}}} = \dot{\lambda}_{\mathrm{N}}^{\omega} \tag{15}$$

$$\dot{r}_{\mathrm{N}} = -\dot{\lambda}_{\mathrm{N}}^{\omega} \frac{\partial f_{\mathrm{N}}^{\omega}}{\partial R_{\mathrm{N}}} = -\dot{\lambda}_{\mathrm{N}}^{\omega}. \tag{16}$$

The consistency condition for the plastic yield function can then be written as follows

$$\dot{f}_{\mathrm{N}}^{p} = \dot{\sigma}_{\mathrm{N}} \frac{\partial f_{\mathrm{N}}^{p}}{\partial \sigma_{\mathrm{N}}} + \dot{X}_{\mathrm{N}} \frac{\partial f_{\mathrm{N}}^{p}}{\partial X_{\mathrm{N}}} + \dot{Z}_{\mathrm{N}} \frac{\partial f_{\mathrm{N}}^{p}}{\partial Z_{\mathrm{N}}} = 0. \tag{17}$$

By substituting evolution equations into the consistency condition the plastic multiplier can be obtained

$$\dot{\lambda}_{\mathrm{N}}^{p} = \frac{E_{\mathrm{N}}\, \dot{\varepsilon}_{\mathrm{N}} \operatorname{sign}(\sigma_{\mathrm{N}} - X_{\mathrm{N}})}{E_{\mathrm{N}} + K_{\mathrm{N}} + \gamma_{\mathrm{N}} \left[1 + m\, X_{\mathrm{N}} \operatorname{sign}(\sigma_{\mathrm{N}} - X_{\mathrm{N}})\right]}. \tag{18}$$

In a similar way the damage multiplier can be obtained as

$$\dot{\lambda}_{\mathrm{N}}^{\omega} = 1 - \frac{1}{1 + A_{\mathrm{d}}(Y_{\mathrm{N}} - Y_{0})}. \tag{19}$$

The illustration of the uniaxial normal behavior at the microplane level is presented in Fig. 3. The tensile behavior governed by the damage is depicted in Fig. 3a, for different values of the brittleness parameter A_{d}. On the other hand, the plastic behavior under compression is shown in Fig. 3b, for different cases of hardening.

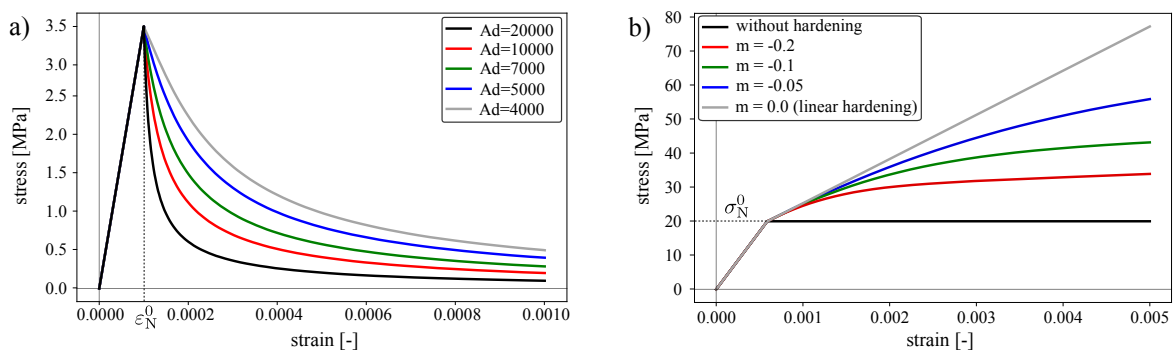

Figure 3: The uniaxial normal behavior at the microplane level: a) tensile damage (TD) for different values of the brittleness parameter A_d; b) compressive plasticity (CP) for different hardening cases

Tangential microplane constitutive law: In this modeling approach we assume that the tangential cumulative damage is the fundamental source of fatigue damage and introduce the tangential microplane behavior in similar way to the pressure sensitive bond interface model with fatigue damage driven by cumulative inelastic slip presented in [11]. The thermodynamic potential of the tangential direction is given as

$$\rho\psi_\mathrm{T}^\mathrm{mic} = \frac{1}{2}(1-\omega_\mathrm{T})E_\mathrm{T}(\boldsymbol{\varepsilon}_\mathbf{T} - \boldsymbol{\varepsilon}_\mathbf{T}^{\boldsymbol{\pi}}) \cdot (\boldsymbol{\varepsilon}_\mathbf{T} - \boldsymbol{\varepsilon}_\mathbf{T}^{\boldsymbol{\pi}}) + \frac{1}{2}K_\mathrm{T} z_\mathrm{T}^2 + \frac{1}{2}\gamma_\mathrm{T}\boldsymbol{\alpha}_\mathbf{T} \cdot \boldsymbol{\alpha}_\mathbf{T} \tag{20}$$

where $\psi_\mathrm{T}^\mathrm{mic}$ is the Helmholtz free energy of the tangential direction, the tangential elastic stiffness is E_T, K_T and γ_T are the isotropic and kinematic hardening moduli respectively. The thermodynamic internal variables are the inelastic tangential strain vector/sliding strain vector defining the irreversible strain $\varepsilon_\mathrm{T}^\pi$, damage variable ω_T ranging from 0 to 1, the internal variables of isotropic hardening z_T and kinematic hardening vector α_T. The thermodynamic forces are obtained by differentiating the thermodynamic potential (20) with respect to each internal variable as follows

$$\boldsymbol{\sigma}_\mathbf{T} = \frac{\partial \rho\psi_\mathrm{T}}{\partial \boldsymbol{\varepsilon}_\mathbf{T}} = (1-\omega_\mathrm{T})E_\mathrm{T}(\boldsymbol{\varepsilon}_\mathbf{T} - \boldsymbol{\varepsilon}_\mathbf{T}^{\boldsymbol{\pi}}) \tag{21}$$

$$\boldsymbol{\sigma}_\mathbf{T}^{\boldsymbol{\pi}} = -\frac{\partial \rho\psi_\mathrm{T}}{\partial \boldsymbol{\varepsilon}_\mathbf{T}^{\boldsymbol{\pi}}} = (1-\omega_\mathrm{T})E_\mathrm{T}(\boldsymbol{\varepsilon}_\mathbf{T} - \boldsymbol{\varepsilon}_\mathbf{T}^{\boldsymbol{\pi}}) \tag{22}$$

$$\boldsymbol{X}_\mathrm{T} = \frac{\partial \rho\psi_\mathrm{T}}{\partial \boldsymbol{\alpha}_\mathbf{T}} = \gamma_\mathrm{T}\boldsymbol{\alpha}_\mathrm{T} \tag{23}$$

$$Z_\mathrm{T} = \frac{\partial \rho\psi_\mathrm{T}}{\partial z_\mathrm{T}} = K_\mathrm{T} z_\mathrm{T} \tag{24}$$

$$Y_\mathrm{T} = \frac{\partial \rho\psi_\mathrm{T}}{\partial \omega_\mathrm{T}} = \frac{1}{2}E_\mathrm{T}(\boldsymbol{\varepsilon}_\mathbf{T} - \boldsymbol{\varepsilon}_\mathbf{T}^{\boldsymbol{\pi}}) \cdot (\boldsymbol{\varepsilon}_\mathbf{T} - \boldsymbol{\varepsilon}_\mathbf{T}^{\boldsymbol{\pi}}). \tag{25}$$

The effective sliding stress can be written as

$$\tilde{\boldsymbol{\sigma}}_\mathbf{T}^{\boldsymbol{\pi}} = \frac{\boldsymbol{\sigma}_\mathbf{T}^{\boldsymbol{\pi}}}{1-\omega_\mathrm{T}} = E_\mathrm{T}(\boldsymbol{\varepsilon}_\mathbf{T} - \boldsymbol{\varepsilon}_\mathbf{T}^{\boldsymbol{\pi}}). \tag{26}$$

The threshold function is defined similarly to plasticity theory and including the sensitivity to the lateral pressure

$$f_{\mathrm{T}} = \left\| \tilde{\boldsymbol{\sigma}}^{\boldsymbol{\pi}}_{\mathbf{T}} - \boldsymbol{X}_{\mathbf{T}} \right\| - Z - \sigma^0_{\mathrm{T}} + a\, \sigma_N \tag{27}$$

where $\|.\|$ defining the norm of the vector, σ^0_{T} the tangential reversibility limit, σ_N is the normal microplane stress, and a is the pressure sensitivity parameter. The non associative flow potentials defined as

$$\phi_{\mathrm{T}} = f_{\mathrm{T}} + \frac{S(1-\omega_{\mathrm{T}})^c}{(r+1)} \left(\frac{\sigma^0_{\mathrm{T}}}{\sigma^0_{\mathrm{T}} - a\, \sigma_N} \right) \left(\frac{Y_{\mathrm{T}}}{S} \right)^{r+1} \tag{28}$$

The evolution equations can be obtained as

$$\dot{\boldsymbol{\varepsilon}}^{\boldsymbol{\pi}}_{\mathbf{T}} = \dot{\lambda}^{\pi}_{\mathrm{T}} \frac{\partial \phi_{\mathrm{T}}}{\partial \boldsymbol{\sigma}^{\boldsymbol{\pi}}_{\mathbf{T}}} = \frac{\dot{\lambda}^{\pi}_{\mathrm{T}}}{1-\omega_{\mathrm{T}}} \frac{\tilde{\boldsymbol{\sigma}}^{\boldsymbol{\pi}}_{\mathbf{T}} - \boldsymbol{X}_{\mathbf{T}}}{\left\| \tilde{\boldsymbol{\sigma}}^{\boldsymbol{\pi}}_{\mathbf{T}} - \boldsymbol{X}_{\mathbf{T}} \right\|} \tag{29}$$

$$\dot{z}_{\mathrm{T}} = -\dot{\lambda}^{\pi}_{\mathrm{T}} \frac{\partial \phi_T}{\partial Z_{\mathrm{T}}} = \dot{\lambda}^{\pi}_{\mathrm{T}} \tag{30}$$

$$\dot{\boldsymbol{\alpha}}_{\mathbf{T}} = -\dot{\lambda}^{\pi}_{\mathrm{T}} \frac{\partial \phi_{\mathrm{T}}}{\partial \boldsymbol{X}_{\mathbf{T}}} = \dot{\lambda}^{\pi}_{\mathrm{T}} \frac{\tilde{\boldsymbol{\sigma}}^{\boldsymbol{\pi}}_{\mathbf{T}} - \boldsymbol{X}}{\left\| \tilde{\boldsymbol{\sigma}}^{\boldsymbol{\pi}}_{\mathbf{T}} - \boldsymbol{X} \right\|} \tag{31}$$

$$\dot{\omega}_{\mathrm{T}} = \dot{\lambda}^{\pi}_{\mathrm{T}} \frac{\partial \phi_{\mathrm{T}}}{\partial Y_{\mathrm{T}}} = (1-\omega_{\mathrm{T}})^c \left(\frac{\sigma^0_{\mathrm{T}}}{\sigma^0_{\mathrm{T}} - a\, \sigma_N} \right) \left(\frac{Y_{\mathrm{T}}}{S} \right)^r \dot{\lambda}^{\pi}_{\mathrm{T}}. \tag{32}$$

In analogy to the normal direction, the sliding multiplier can be obtained

$$\dot{\lambda}^{\pi}_{\mathrm{T}} = \frac{E_{\mathrm{T}}\, \dot{\boldsymbol{\varepsilon}}_{\mathbf{T}} \cdot\, (\tilde{\boldsymbol{\sigma}}^{\boldsymbol{\pi}}_{\mathbf{T}} - \boldsymbol{X}) / \left\| \tilde{\boldsymbol{\sigma}}^{\boldsymbol{\pi}}_{\mathbf{T}} - \boldsymbol{X} \right\|}{E_{\mathrm{T}}/(1-\omega_{\mathrm{T}}) + K_{\mathrm{T}} + \gamma_{\mathrm{T}}}. \tag{33}$$

To illustrate the proposed cumulative sliding behavior of tangential microplane direction, an elementary example of the tangential stress - strain relationship under monotonic and cyclic strain controlled loading is depicted in Fig. 4a showing the degradation of the stress under cyclic loading. The corresponding evolution of the damage is shown in Fig. 4b. This behavior is essential for the model to include the fatigue damage owing to the internal frictional sliding.

2.3 Homogenization

The homogenization approach introduced by [9] based on the principle of energy equivalence is used for the damage in this study. This principle works with the effective stress and strain tensors $\tilde{\boldsymbol{\varepsilon}}, \tilde{\boldsymbol{\sigma}}$. These effective quantities reflect the condition of the undamaged material and the relation between the effective strain and stress tensors can be written as follows

$$\tilde{\boldsymbol{\sigma}} = \boldsymbol{D}^{\mathrm{e}} : \tilde{\boldsymbol{\varepsilon}}, \tag{34}$$

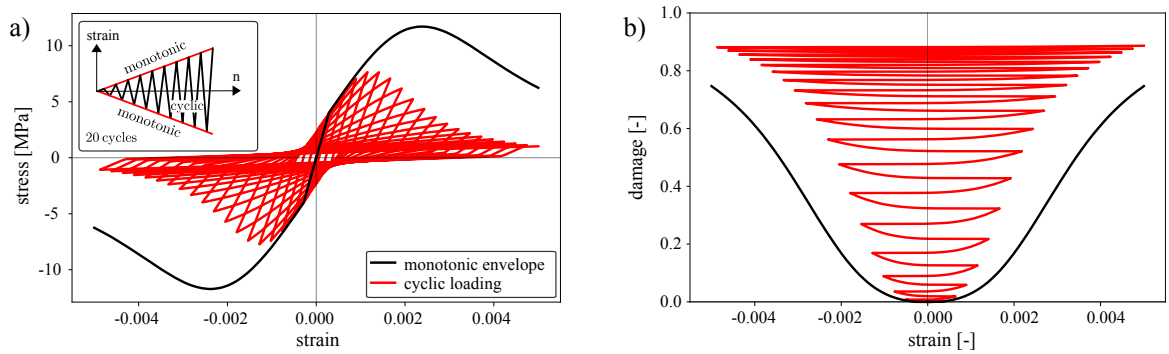

Figure 4: The tangential behavior at the microplane level (CSD): a) monotonic and cyclic stress-strain relationship; b) the corresponding damage evolution

where $\boldsymbol{D}^{\mathrm{e}}$ is the fourth order elastic stiffness tensor. The relation between the macroscopic stress tenser $\boldsymbol{\sigma}$ and the effective stress tensor $\tilde{\boldsymbol{\sigma}}$ is given as follows

$$\boldsymbol{\sigma} = \boldsymbol{\beta} : \tilde{\boldsymbol{\sigma}}, \tag{35}$$

where $\boldsymbol{\beta}$ is the fourth order damage inverse/integrity tensor. The relation between the effective strain tensor $\tilde{\boldsymbol{\varepsilon}}$ and the macroscopic strain tensor $\boldsymbol{\varepsilon}$ is given as

$$\tilde{\boldsymbol{\varepsilon}} = \boldsymbol{\beta}^{\mathrm{T}} : \boldsymbol{\varepsilon}. \tag{36}$$

By substituting (34) and (36) into (35) we can write

$$\boldsymbol{\sigma} = \boldsymbol{\beta} : \tilde{\boldsymbol{\sigma}} = \boldsymbol{\beta} : \boldsymbol{D}^{\mathrm{e}} : \tilde{\boldsymbol{\varepsilon}} = \boldsymbol{\beta} : \boldsymbol{D}^{\mathrm{e}} : \boldsymbol{\beta}^{\mathrm{T}} : \boldsymbol{\varepsilon}, \tag{37}$$

therefore the secant stiffness tensor is obtained as

$$\boldsymbol{D} = \boldsymbol{\beta} : \boldsymbol{D}^{\mathrm{e}} : \boldsymbol{\beta}^{\mathrm{T}}. \tag{38}$$

The fourth order inverse damage tensor can be written as

$$\beta_{ijkl} = \frac{1}{4}(\phi_{ik}\delta_{jl} + \phi_{il}\delta_{jk} + \phi_{jk}\delta_{il} + \phi_{jl}\delta_{ik}), \tag{39}$$

In this modeling approach we assume that the tensile behavior is governed by the normal microplane damage, and the compressive behavior is governed by the plastic normal behavior and the cumulative sliding damage.

The second order integrity tensor $\boldsymbol{\phi}$ and the elastic stiffness tensor are given as

$$\phi_{ij} = \frac{3}{2\pi}\int_{\Omega} \phi^{\mathrm{mic}}\, n_i n_j d\Omega = \frac{3}{2\pi}\int_{\Omega} \sqrt{(1-\omega^{\mathrm{mic}}(n))}\, n_i n_j d\Omega, \tag{40}$$

$$\boldsymbol{D}^{\mathrm{e}}_{ijkl} = \lambda\delta_{ij}\delta_{ij} + \mu(\delta_{ik}\delta_{jl} + \delta_{il}\delta_{jk}). \tag{41}$$

Plastic strain tensor: According to [12] the macroscopic plastic strain tensor can be obtained as the integral of the microplane plastic strains as follows

$$\varepsilon^{p}_{ij} = \frac{3}{2\pi}\int_{\Omega} \varepsilon^{p,\mathrm{mic}}_{N} n_i n_j d\Omega + \frac{3}{2\pi}\int_{\Omega} \frac{\varepsilon^{\pi,\mathrm{mic}}_{Tr}}{2}(n_i\delta_{rj} + n_j\delta_{ri}) d\Omega. \tag{42}$$

Macroscopic stress tensor: The macroscopic stress tensor can be obtained as follows

$$\boldsymbol{\sigma} = \boldsymbol{\beta} : \boldsymbol{D}^{\mathrm{e}} : \boldsymbol{\beta}^{\mathrm{T}} : (\boldsymbol{\varepsilon} - \boldsymbol{\varepsilon}^{P}). \tag{43}$$

3 ELEMENTARY STUDY OF THE MODEL RESPONSE

To study and evaluate the model behavior under elementary loading conditions simulations at the level of a single material have been conducted. As emphasized in [8], single material point simulations are important to verify the fundamental model behavior and to calibrate the model parameters. A benchmark test data for different concrete types from the literature are used to evaluate the model response. For this analysis, the numerical integration over the hemisphere has been performed with $n_{\mathrm{mp}} = 28$ number of microplanes.

Fig. 5a, shows the simulation with parameters adjusted to fit the uniaxial compression test data presented by [13]. Another simulation shown in Fig. 5b presents the fit for uniaxial tension test data presented by [14]. The biaxial failure envelope test data reported in [15] is depicted in Fig. 5c and compared with the numerical results obtained by the model.

The cyclic uniaxial compression test data presented by [16] is depicted in Fig. 6b. The response obtained using the numerical model is shown in Fig. 6a together with the calculated monotonic envelope. The areas of the obtained hysteretic loops representing

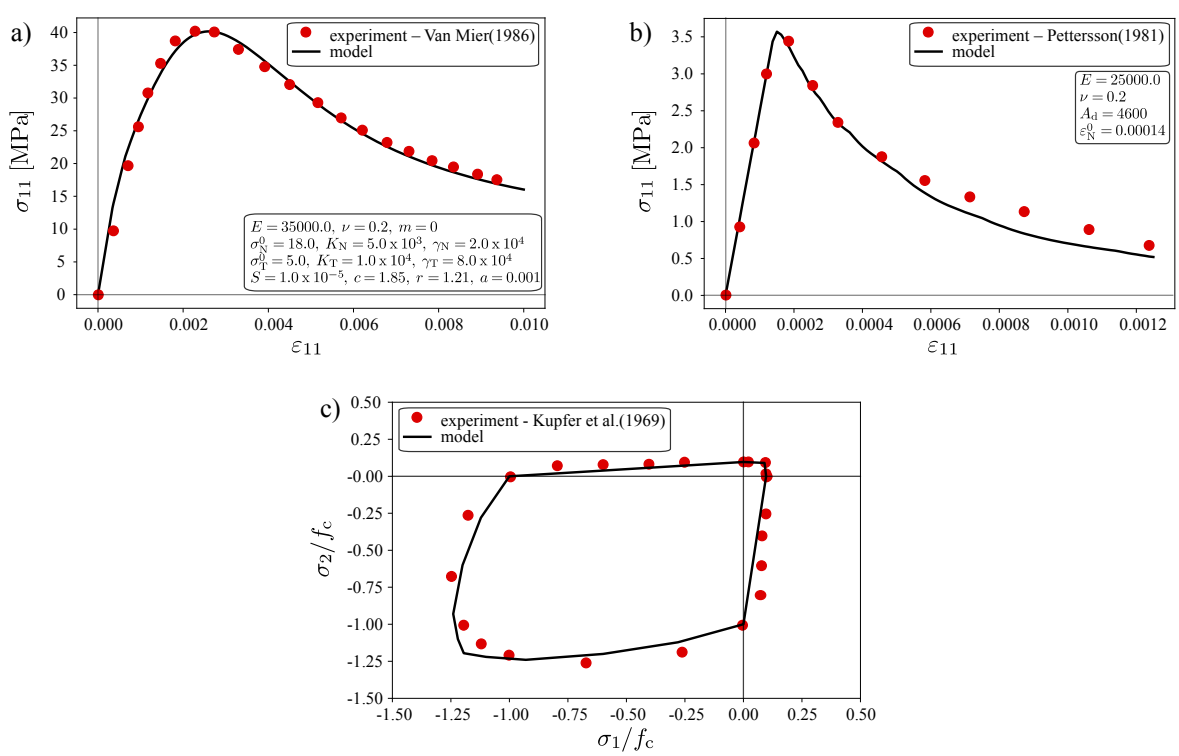

Figure 5: Elementary study of the model behavior under monotonic loading with comparison to experimental results: a) uniaxial compression ; b) uniaxial tension; c) biaxial failure envelope

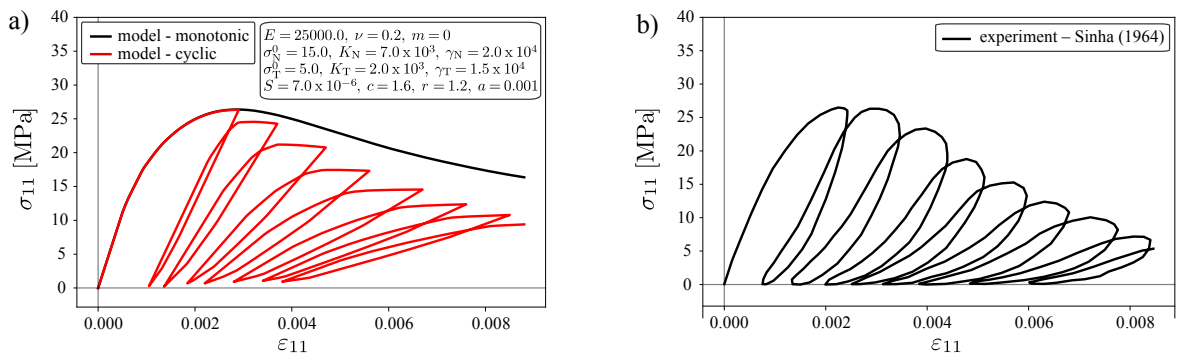

Figure 6: Elementary study of the model behavior under cyclic loading with comparison to experimental results; a) results obtained by the model; b) experimental results

the dissipated energy during the cyclic loading history show an acceptable agreement with experimental results. The numerical results show progressive degradation of the compressive stress during the cyclic loading. The comparison to the monotonic envelope reveals the accumulation of the damage governed by the internal sliding, which is essential aspect for modeling of the fatigue behavior of concrete.

To elucide the internal structure of the introduced model, an elementary example of the model behavior exposed to compressive fatigue strain loading is depicted in Fig. 7. In the example, the parameters obtained from the uniaxial compression test shown in Fig. 5a have been used. The stress-strain relationship for the monotonic and fatigue loading with four different strain ranges up to 100 cycles is shown in Fig. 7a. The corresponding compressive stress decrease at maximum stain over cycles "fatigue relaxation curve" for the different cases is presented in Fig. 7b. It shows rapid decay of the compressive stress for the increased loading range. These curves show that the model can capture the degradation of the material during the cycling. This aspect is essential for fatigue modeling showing the degradation of the material strength due to the fatigue loading. The microplane sliding damage evolution at each microplane for the different four loading ranges is depicted in Fig. 7c, showing that for the largest loading range plotted in the blue color, the sliding damage has propagated in a larger number of microplanes in comparison to the other loading ranges.

4 CONCLUSIONS

The proposed microplane model is formulated within the thermodynamic framework of the microplane constitutive laws. The key idea of the proposed model is to relate the fatigue damage to a cumulative inelastic sliding stains introduced at the microplane level. The initial study of proposed model showing acceptable description the elementary test data for concrete in the literature. The introduced cumulative sliding damage at the microplane level as fatigue damage source presents a good chance to describe the fatigue behavior of concrete under compression loading. Further systematic calibration and validation procedures of the model with regularization technique will be conducted in the future.

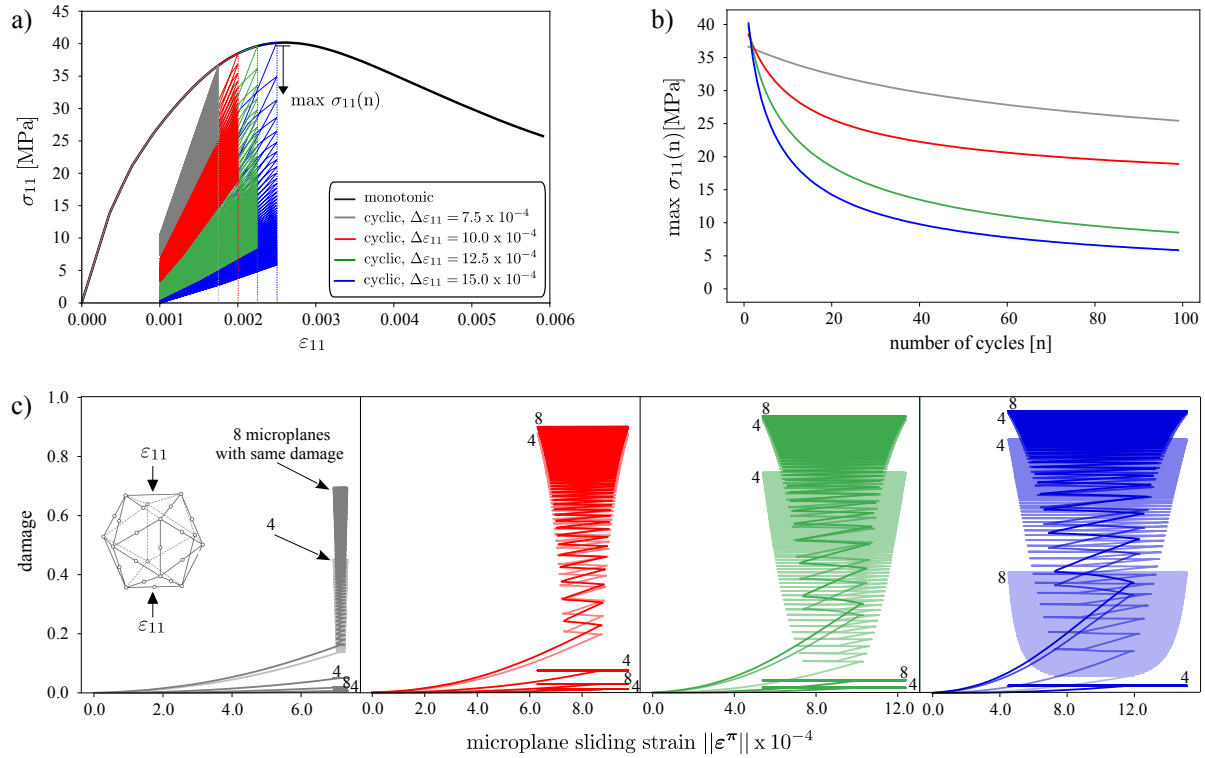

Figure 7: Example of the model behavior under compressive fatigue loading - strain controlled: a) stress-strain relationship ; b) decease of the compressive stress with the number of cycles; c) sliding damage for different microplanes

Acknowledgment

The work was supported by the Federal Ministry for Economic Affairs and Energy (BMWi 0324016C), project number F-2013-021. This support is gratefully acknowledged.

REFERENCES

[1] D. Pfanner, Zur degradation von stahlbetonbauteilen unter ermüdungs-beanspruchung. konstruktiven ingenieurbau. Ruhr-universiät bochum (2003).

[2] J. Marigo, Modelling of brittle and fatigue damage for elastic material by growth of microvoids,Engineering Fracture Mechanics,21(4)(1985) 861-874.

[3] A. Alliche, Damage model for fatigue loading of concrete, International Journal of Fatigue,26(9)(2004) 915-921.

[4] V. M. Kindrachuk, M. Thiele, J. F. Unger, Constitutive modeling of creep-fatigue interaction for normal strength concrete under compression, International Journal of Fatigue,78(2015)81-94.

[5] R. Desmorat, F. Ragueneau, H. Pham, Continuum damage mechanics for hysteresis and fatigue of quasi-brittle materials and structures, International Journal for Numerical and Analytical Methods in Geomechanics 31(2)(2007)307-329.

[6] K. Kirane, Z. P. Bažant, Microplane damage model for fatigue of quasibrittle materials: Sub-critical crack growth, lifetime and residual strength, International Journal of Fatigue 70 (2015)93-105.

[7] Caner, F.C., Bažant, Z.P., 2013a. Microplane Model M7 for Plain Concrete. I: Formulation. Journal of Engineering Mechanics 139, 1714-1723.

[8] Caner, F.C., Bažant, Z.P., 2013b. Microplane Model M7 for Plain Concrete. II: Calibration and Verification. Journal of Engineering Mechanics 139,1724-1735.

[9] Jirasek, M., 1999. Comments on Microplane Theory, in: Mechanics of Quasibrittle Materials and Structures.Hermes Science Publications, pp. 55-77.

[10] F. Ragueneau, N. Dominguez, A. Ibrahimbegovic, Thermodynamic-based interface model for cohesive brittle materials: Application to bond slip in RC structures, Computer Methods in Applied Mechanics and Engineering 195 (52)(2006) 7249-7263.

[11] Baktheer, A., Chudoba, R.: Modeling of bond fatigue in reinforced concrete based on cumulative measure of slip, Computational Modeling of Concrete and Concrete Structures, pp.767-776, Editors: Meschke, G., et al., EURO-C, Bad Hofgastein,2018

[12] Ignacio Carol and Zdeněk P. Bažant. Damage and plasticity in microplane theory. In:International Journal of Solids and Structures34.29 (1997), pp 3807-3835.

[13] Van Mier and Jan G. M., Multiaxial strain-softening of concrete, Materials and Structures (1986),19-3, PP 1871-6873, issn:1871-6873.

[14] Petersson, Per-Erik, Crack growth and development of fracture zones in plain concrete and similar materials (1981), Division, Inst.

[15] Kupfer, Helmut and Hilsdorf, Hubert K and Rusch, Hubert, Behavior of concrete under biaxial stresses, Journal Proceedings (1969),66-8, PP 656-666.

[16] Sinha, BP and Gerstle, Kurt H and Tulin, Leonard G, Hubert K and Rusch, Hubert, Stress-strain relations for concrete under cyclic loading, Journal Proceedings (1964),61-2, PP 195-212.